Tellus
SERIES A
DYNAMIC
METEOROLOGY
AND OCEANOGRAPHY
PUBLISHED BY THE INTERNATIONAL METEOROLOGICAL INSTITUTE IN STOCKHOLM

Tellus (2010), 62A, 605–616
Printed in Singapore. All rights reserved

TELLUS

Extreme rainfall events in southern Sweden: where does the moisture come from?

By MALIN GUSTAFSSON*, DAVID RAYNER and DELIANG CHEN, *Department of Earth Sciences, University of Gothenburg, PO Box 460, 405 30 Gothenburg, Sweden*

(Manuscript received 23 September 2009; in final form 11 March 2010)

ABSTRACT

The atmospheric transport of moisture leading to extreme summer precipitation events in southern Sweden was investigated using a Lagrangian trajectory model. Surprisingly, we found that the trajectories crossed continental Europe and the Baltic Sea before arriving over Sweden; they did not arrive directly from the North Sea. Such transport pathways were not seen for a control sample of non-extreme rainfall events. We then used a new source region identification technique to investigate the hypothesis that Europe and the Baltic are important sources of the moisture that is rained out in the extreme events. Although the results varied between events, we found that this is indeed the case. Our results establish the atmospheric transport patterns that are apparently a pre-requisite for extreme rainfall events to occur in southern Sweden, and further suggest regional moisture availability may also play a key role.

1. Introduction

1.1. Extreme precipitation events in Sweden

Flooding caused by widespread, heavy rainfall can result in lost lives, damage to property and infrastructure and cause severe socio-economic disruption. For an extreme precipitation event to occur, a number of factors must occur in combination. Unless there is sufficient moisture available for convective thunderstorm activity to develop due to solar heating, sufficient quantities of moisture must be advected into the region before an uplift mechanism initiates precipitation. Moisture advection in turn requires that a suitable region of evaporation (a *source region*) exist, from which moisture can be transported. If any of these components is absent—no source region, wrong transport path or no uplift—then extreme precipitation cannot occur.

Serious floods do occur in Sweden. After a dry period in the 1970s, Sweden has been subjected to a series of floods in the last 15 years (Lindström and Bergström, 2004) with floods in 1993, 1995, 1998 and two events in 2000. An emerging concern in Sweden is that extensive regulation of rivers for hydro-power has caused society to be over-confident with respect to flood risk, as demonstrated by development on land that previously was regularly flooded (Räddningsverket, 2000). After the rainfall in 2000, the water level in the large Lake Vänern reached the highest level since it was regulated in 1938 (Lindström and Bergström, 2004), and it was subsequently decided to lower the Lake's water level.

Increases in the frequency or severity of extreme rainfall under climate change conditions would require significant adaptation measures in Sweden. It is difficult to make concrete statements about whether this is likely to happen, however, because the critical factors that lead to extreme events in Sweden are not known. Climatological studies show that frontal activity is important for extreme precipitation under non-cyclonic conditions (Hellström and Malmgren, 2004), but extreme precipitation in Sweden occurs predominantly under cyclonic atmospheric circulation types (Hellström, 2005). The discriminatory power of the latter observation is limited, however, because the cyclonic type is the most frequently observed type over southern Sweden (Linderson et al., 2004).

Hellström (2005) also found that extreme events tended to be favoured by southerly winds, and weaker westerly winds. She hypothesized that weaker westerly winds may promote extreme events by allowing rain-producing systems to persist for longer times, or that the Baltic Sea may be an important source region for the moisture that rains out in the events. However, detailed information about atmospheric moisture transport and source regions is required to investigate such hypotheses, which cannot be provided by climatological studies. The purpose of our paper is to address this deficiency.

1.2. Atmospheric water vapour transport

It is important to realize that the transport of water vapour in the atmosphere (Newell et al., 1992), and the source–receptor

*Corresponding author.
e-mail: malin.s.gustafsson@gmail.com
DOI: 10.1111/j.1600-0870.2010.00456.x

relationship between regions of evaporation and precipitation, is still poorly understood. The water vapour lost during a precipitation event may have evaporated from a water surface, come from biomass transpiration or even from evaporation of falling hydrometeors, and may have a local origin or have been transported thousands of kilometres (Trenberth et al., 2003). According to Trenberth (1998), less than a third of the water rained out in extratropical storm systems had been evaporated locally—rather, most of the moisture is transported in to the storm system from outside sources. Eckhardt et al. (2004) showed that extratropical cyclones with strongly developed warm conveyor belts—moist airstreams which rise from the boundary layer to the upper troposphere ahead of the surface cold front—are responsible for much of the poleward moisture transport by extratropical cyclones. Finally, the ratio of moisture originating from local versus distant sources differs considerably between seasons (Trenberth, 1999); in winter, local moisture availability is low and hence large-scale transport is most important, whereas the recycling of precipitation increase in importance in summer.

There are several possible ways to estimate the moisture source regions that contribute to extreme events, and the transport paths involved. For instance, if a sample of the rainwater is available the oxygen and hydrogen isotopic ratios could be measured and compared with an estimate for the assumed source region (e.g. Weyhenmeyer et al., 2002). This technique has a significant drawback as it requires an analysis of a rain sample, hence making it impossible to examine past events for which no samples are available. Another method is to simulate precipitation events using a general circulation model (GCM) based on the Eulerian equation. For example, Keil et al. (1999) analysed the moisture transport during an extreme precipitation event in the Czech Republic and southern Poland in the summer of 1997 by re-running a high-resolution forecast model over a limited area. Bosilovich and Schubert (2002) further developed this method by including constituent tracers of local water vapour sources into the simulation.

1.3. Lagrangian trajectory modelling

Trajectory modelling is a Lagrangian alternative to the Eulerian tracer approach. The trajectory of a very small parcel of air (or particle) is calculated by solving Lagragne's equation, which is the same as finding the path that minimizes the integral of the Lagrangian over time (Stohl, 1998). The trajectory approach relies solely on analysed wind field data. Lagrangian models provide an efficient way to calculate the dispersion of pollutants or tracers from—or the advection towards—a single location. For simple analyses, Lagrangian models without numerical diffusion can be used. A further practical consideration is that Eularian models generally require that emission sources be defined at a resolution comparable to the computational grid, whereas Lagrangian models can use emissions sources with any resolution (Draxler and Hess, 1998). For the past few decades, trajectory models such as The Hybrid Single-Particle Lagrangian Integrated Trajectory (HYSPLIT, Draxler and Rolph, 2003) and FLEXTRA (Stohl et al., 1995) have frequently been used to analyse the transport path of atmospheric constituents such as air pollutants, greenhouse gases or radioactive constituents from the source to the receptor site (e.g. Stohl et al., 2003; Tang et al., 2009). The model is usually run backwards in time to determine the source of the species of interest (Stohl et al., 1995).

Trajectory modelling allows air parcels to be tracked backwards in time from an extreme precipitation event, and so can provide information about the transport paths involved. Changes in the physical properties of the air parcel can also be calculated; in particular, changes in the moisture content provide an estimate of where the source region evaporation occurred. This technique is well established, and can provide detailed information about the moisture source regions and transport paths leading to extreme events. For example, James et al. (2004) used Lagrangian trajectory modelling to determine that, for a flooding event in Germany on the 11–13 August 2002, during the early stages of the episode the main moisture source region was the Mediterranean, whereas towards the end of the event the principal source of moisture was evaporation from the land surface in Eastern Europe and the Black Sea. A similar approach was used by Stohl et al. (2008), who analysed an episode of very heavy precipitation in western Norway which resulted in loss of life and severe infrastructural damage. They were able to show that the episode was triggered by two tropical hurricanes that had transitioned into extra-tropical cyclones. These generated a so-called atmospheric moisture conveyer belt—a large stream of moist air—which in this case extended over more than 40° of latitude and across the North Atlantic. Trajectory modelling has also been used to trace the path of moisture from the troposphere to the stratosphere (Jackson et al., 1998), and to simulate Antarctic snow pit records (Helsen et al., 2006).

There are several other case studies that identify moisture source regions associated with severe precipitation events (e.g. Massacand et al., 1998; Reale et al., 2001). Single-case studies such as these may give an insight into specific events, but the lack of replication makes it difficult to make any general conclusions. To do this, one must analyse a larger number of extreme events in one region, and try to identify any patterns.

In this study, we have analysed 21 extreme precipitation events from southern Sweden using trajectory modelling. An ensemble of trajectory paths was calculated for each event. We initially examined the trajectories quantitatively, and found that many air parcels associated with precipitation were transported across Europe and the Baltic Sea. This pattern was not seen in the trajectories that contributed to rainfall in a control-group of non-extreme events. We then hypothesized that the reason such trajectory paths are associated with extreme events is that local moisture uptake in these regions plays an important role. To test this hypothesis, we devised a novel source region identification system based on changes in specific humidity along trajectories.

This enabled us to define the geographic extent of the source region for each extreme event using the ensemble of trajectory paths, and to determine the relative importance of long and short distance moisture transport.

2. Precipitation data and the HYSPLIT trajectory model

Precipitation occurs throughout the year in Sweden, mainly as a result of the characteristic atmospheric westerly flow and the close proximity to the Atlantic Ocean. However, the summer season usually experiences more intense precipitation that any other season—approximately 85% of the heavy precipitation events occur during this period (Alexandersson and Vedin, 2005)—so we restricted our study to June to August.

The region of interest (hereafter referred to as the "target region") was centred on 15° longitude and 57.5° latitude, with a size of 3.75° longitude and 2.5° latitude (Fig. 1). This region was selected due to its relatively uniform precipitation patterns and topography, making it likely that the moisture precipitated here originates from similar sources. The west coast of Sweden was excluded as it has a quite different precipitation pattern (Alexandersson, 2006). The target region consists mostly of hill and lowland terrain, with a maximum elevation of 377 m above sea level.

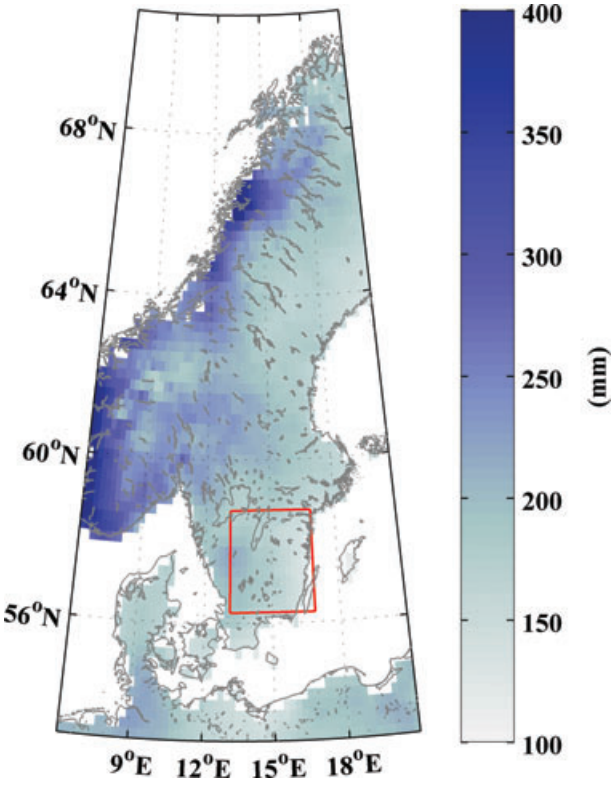

Fig. 1. Map of the study area. The target region in southern Sweden is marked with a square. The raster shows average summer (June–July–August) precipitation, 1961–1990, from the E-OBS data set (Haylock et al., 2008).

2.1. Extreme precipitation events

Rainfall intensity in Sweden is lower than in many parts of the world, with annual-average 1-day maximum precipitation generally between 25 and 40 mm (Achberger and Chen, 2006). The Swedish Meteorological and Hydrological Institutes (SMHI) define an extreme precipitation event to be 40 mm of rain in the 24 hr, because above this limit there is an increasing risk of flooding of rivers and landslides (Alexandersson, 2006). In our study, we used daily (24 hr totals recorded at 0700 local time) observed data from SMHI stations to identify the extreme events. For a day to be classified as an extreme precipitation event, we required that at least five SMHI stations recorded extreme precipitation within the target region. The latter criterion selects against localized extreme events that result from convective activity. Our criteria yielded 21 extreme precipitation events in the target region in the period 1961–2004, which are listed in Table 1. The spatial distribution of the extreme events is shown in Appendix S1 in Supporting Information.

2.1.1. Non-extreme precipitation events. During the course of this study it became clear that we required not only a sample of extreme precipitation events, but also a sample of non-extreme precipitation events to use as a control-group with which the extreme events could be compared. Although there are clearly a very large number of days with non-extreme rainfall, many have very different atmospheric conditions to days where extreme rainfall occurs, and so any comparison might be meaningless. What we needed was a sample of days where conditions were similar to those typical of extreme precipitation events, but no extreme precipitation occurred.

As noted in Introduction, Hellström (2005) found that extreme precipitation in Sweden occurs predominantly under cyclonic atmospheric circulation types. Thus, we used the Lamb atmospheric classification system (Lamb 1950; Chen 2000) to derive a control sample. The Lamb system classifies days into 27 classes using geostrophic wind and vorticity derived from MSLP surfaces (see Chen 2000 for details). We calculated Lamb classes for southern Sweden for all days 1961 to 2004 using the NCEP/NCAR reanalysis data set (Kalnay et al., 1996). We grouped the classes into three main categories: cyclonic ("C"), anticyclonic ("A"), and directional ("D"). The classes for the day of each extreme event, and the 2 days preceding, are shown in Table 1.

Twelve of the extreme events occurred on a day with a cyclonic weather class over the target region, and six of these events had persistent cyclonic circulation in the days leading up to the event. Further, the three events with the highest number of stations recording extreme rainfall are among the six with persistent cyclonic weather type (Table 1). Thus, it appears

Table 1. Extreme precipitation events

Event date	Lamb weather class			No. stations
	Day of the event	1 day prior	2 days prior	
1 August 1961	C	A	A	5
14 August 1969	D (E)	D (SE)	A	7
18 August 1970	D (SE)	D (SE)	A (AS)	5
7 August 1971	D (W)	D (SW)	D (SW)	7
13 July 1972	D (N)	D (N)	D (NW)	15
26 July 1972	**C**	**C**	**C**	**6**
3 August 1977	D (SE)	A	A	7
26 August 1979	C	C (E)	D (SW)	10
16 July 1980	**C**	**C**	**C**	**10**
23 June 1984	C	D (W)	D (SW)	8
24 July 1986	C	C	D (SW)	9
16 June 1987	**C**	**C**	**C (SE)**	**23**
23 August 1987	C	D (W)	D (SW)	5
14 July 1988	D (SE)	A	A (SW)	6
19 July 1988	**C**	**C**	**C**	**19**
28 June 1991	**C**	**C**	**C**	**6**
11 July 1993	D (S)	D (S)	D (SW)	18
18 August 1994	D (SE)	A (S)	A	7
15 July 1995	D (SE)	D (SE)	C	6
9 July 1996	**C (NE)**	**C**	**C**	**24**
14 July 1999	C	D (S)	A	5

Columns 2–4 show the Lamb classes (Lamb 1950; Chen 2000) for southern Sweden for the day of the extreme event and the 2 previous days. The main Lamb classes used are C, cyclonic; A, anticyclonic; D, directional flow, with the wind-direction show in parentheses for directional and hybrid classes. The final column indicates how many stations inside the target region recorded extreme precipitation (40 mm 24 hr^{-1} or more) during the day of the event. Events with cyclonic weather class on the day of the even and 2 days prior are shown in bold.

persistent cyclonic circulation represents favourable conditions for extreme rainfall in southern Sweden in summer (June–August).

A sample of 10 non-extreme summer precipitation events was then selected as a control for the extreme events. The non-extreme events had a minimum of three consecutive days of cyclonic-type weather over the target region leading up to the event, but no precipitation measurement for the whole period could be above 40 mm 24 hr^{-1}, and for the day of the non-extreme rainfall event all values were less than 15 mm 24 hr^{-1}. In addition, an extreme precipitation event could not occur in the three days that followed the non-extreme event. Ten events that fulfilled these criteria were randomly selected from the period 1961 to 2004, and are listed in Table 2.

2.2. *Trajectory Model—HYSPLIT*

The Hybrid Single-Particle Lagrangian Integrated Trajectory (HYSPLIT) 4.0 model (Draxler, 2003) was used to produce back-trajectories. HYSPLIT was run with meteorological analysed fields from the ERA40 project from the European Centre for Medium-Range Weather Forecasts (ECMWF). The meteorological fields that we used had been interpolated from ERA40's native resolution onto a 0.5° horizontal resolution grid with 23 vertical pressure levels extending between 1 and 1000 hPa.

Backwards trajectory modelling is very sensitive to initial conditions, and particles "released" at slightly different times or locations may result in very different trajectories. This can be true even if the locations of the different release points correspond to the same grid cell/level in the gridded meteorological wind fields. Thus, trajectory analysis typically involves an ensemble of particles released at different locations, and HYSPLIT can calculate multiple back-trajectories simultaneously. We used a release grid with 10 × 12 horizontal coordinates on 30 vertical levels (giving a total of 3600 release points) to get a good representation of the transport pathways into the target region. The vertical levels were distributed according to atmospheric pressure, with the first level at 10 m above ground level (agl) and the top at 10 420 m agl. From each of the points in the release grid a trajectory was started and run backwards in time for 192 hr (8 days). The 8-day integration time was chosen because James

Table 2. Non-extreme precipitation events

Event date	Lamb weather class		
	Day of the event	1 day prior	2 days prior
28 June 2000	C	C	C
26 June 1997	C	C	C
17 June 1993	C	C (W)	C (NW)
19 July 1991	C	C (W)	C
12 June 1990	C (NE)	C	C
8 June 1989	C	C	C
25 August 1986	C	C	C
19 July 1981	C	C	C
12 August 1979	C	C	C

Columns 2–4 show the Lamb classes for southern Sweden for the day of the extreme event and the 2 previous days, as per Table 1. No precipitation measurement was above 40 mm 24 hr^{-1} for the whole 3-day period, and for the day of the non-extreme rainfall event all values were less than 15 mm 24 hr^{-1}.

et al. (2004) concluded that an 8-day time domain was sufficient to determine the source of moisture contributing to precipitation in Europe. In addition, because the integration period of the observational data was 24 hr, a new set of trajectories were started every third hour, so generating eight sets of trajectories for each release point for each event. The trajectory calculations were restricted to the Northern Hemisphere.

Changes in specific humidity, expressed as grams of water vapour per kilogram of air (including water vapour), were taken to indicate precipitation and evaporation from the air parcel as it moves along its trajectory. Specific humidity is independent of temperature and pressure, and hence it does not change if an air parcel rises to a lower pressure level without losing or gaining water vapour.

3. Experiment 1: qualitative trajectory analysis

3.1. Trajectory paths and vertical profiles

Our first analysis was to qualitatively examine the trajectory ensembles, to identify any similarities in the transport pathways. The very large number of trajectory paths calculated for each event precludes displaying all paths. Instead, the 100 trajectories which lost the largest amount of specific humidity within the target region were selected to represent the trajectories that were likely to have contributed to significant rain inside the target region. These are referred to as 'rain trajectories'.

The rain trajectories for the extreme event on 11 July 1996 are shown, as an example, in Fig. 2. The rain trajectories for a non-extreme event 19 July 1991 are shown in Fig. 3. The paths and vertical profiles for the rain trajectories for all the events are shown Appendix S2 in Supporting Information.

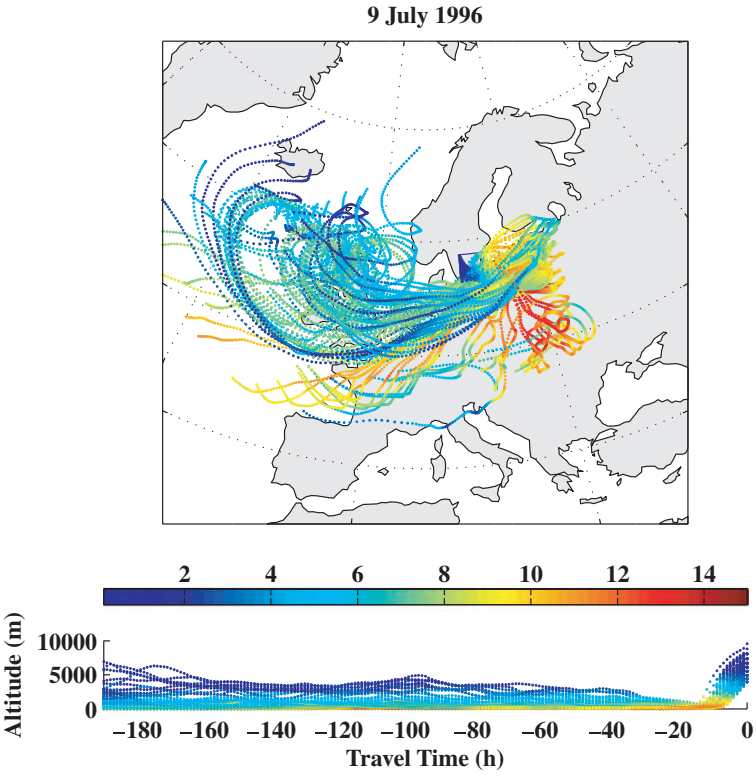

Fig. 2. Rain trajectories (the sub-set of 100 trajectories with the highest loss of specific humidity inside the target region) for the extreme precipitation event on the 9 July 1996. Colour indicates the specific humidity in g kg^{-1}. The upper panel shows the horizontal location of the trajectories and the lower the altitude of the trajectories as a function of time. The time axis shows the trajectory travel time in real-world-time: although the trajectory is calculated with time running backwards (right-to-left), in real-world-time the air parcel begins at –180 hr and arrives at the target at 0 hr. The target region is marked with a blue square.

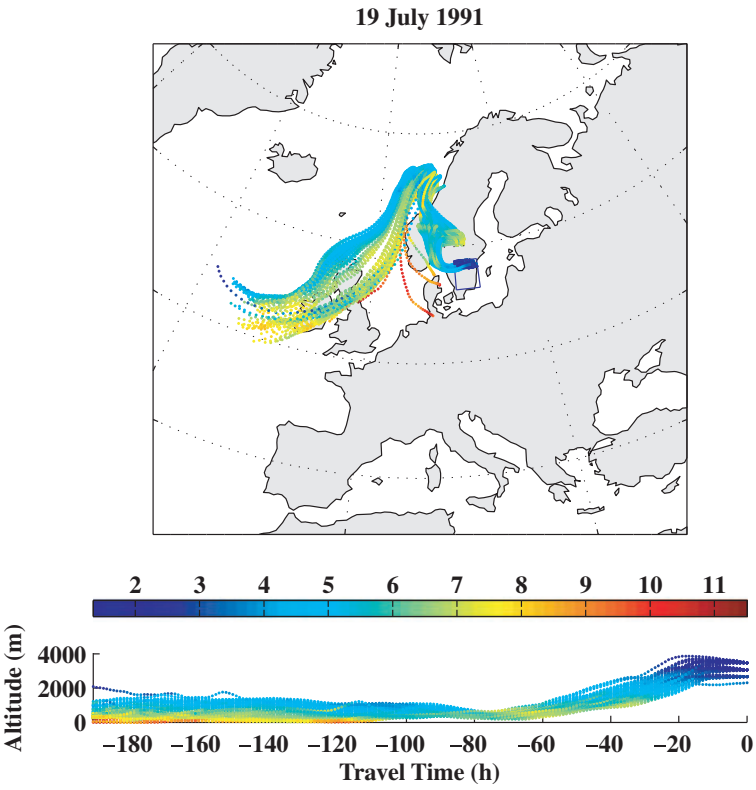

Fig. 3. Rain trajectories (the subset of 100 trajectories with the highest loss of specific humidity inside the target region) for the non-extreme rain event 19 July 1991. See Fig. 2 for further details.

3.2. Discussion

The general vertical profile of the rain trajectories for extreme events is that they come close to the ground, usually within the last 3 days, and then ascend rapidly, losing specific humidity just before arriving at their individual end points. Referring to the example event in Fig. 2, a large portion of the rain trajectories start out 8 days prior to the event at a range of altitudes between 0 and 7000 m, and as time moves forward many rain trajectories increase in altitude and lose specific humidity. But approximately 3 days before the event the rain trajectories start to lose altitude and increase specific humidity as they come closer to the surface. One day prior to the event, the rain trajectories begin to ascend again and specific humidity decreases. This uplift associated with the target region rainfall is clearly displayed by nearly all the rain trajectories. The rain trajectories typically have an end point with an altitude above 1000 m and up to 10 000 m.

The vertical profiles of the rain trajectories for the non-extreme events show these trajectories are often confined to lower altitudes, and have lower end points, than for the extreme events. This is clear from Fig. 3. Some of the rain trajectories for non-extreme events also descend from the upper Troposphere in the week prior to the event.

A detailed investigation of the physical mechanisms that cause particular trajectory pathways to be followed for particular events is beyond the scope of this paper. Many of extreme precipitation events, and all the non-extreme events, are associated with cyclonic weather classes, so it is likely that in many cases the final ascent of the rain trajectories represents the Warm Conveyer Belt component of an extratopical cyclone. Given this, it is tempting to associate the descending path followed by many of the trajectories with the Dry Intrusion component, which descends behind the cold front (Browning, 1997). However, we caution against over-interpreting the descending part of the trajectory path, because in many cases the rain trajectories ascend from with the atmospheric boundary layer; we do not realistically expect that HYSPLIT can accurately trace the path of air parcels through the boundary layer. The trajectory paths may be best viewed as reflecting the large-scale synoptic patterns, rather than the actual paths of "rain-producing" trajectories.

The horizontal profiles of the rain trajectories for the extreme events are more varied, and in many cases more than one dominant transport pathway can be identified. The most striking observation is that, despite the westerly flow that characterizes the region, none of the events are dominated by rain trajectories that come directly in from the North Atlantic and across the North Sea. For 13 of the 21 events, rain trajectories do originate in the North Atlantic or the North Sea, but then follow anti-clockwise pathways in over the British Isles or North Sea, then pass over the northern European continental margin before crossing the Baltic Sea to arrive at the target area from the south or the east.

This profile is shown in Fig. 2. A second major category of events have rain trajectories which begin the 8-day trajectory calculation in Eastern Europe, for example 14 August 1969 and 18 August 1970 and 3 August 1977. A further grouping of trajectories, shown in events 26 July 1972, 15 July 1995 and 14 July 1999 cross the Swedish-Norwegian mountains and follow an anti-clockwise path over the continent before again crossing the Baltic to the target region. Of course, in addition to these general patterns, there are air parcels that have been transported from regions as far away as the west coast of United States during the 8-day period, and others have only been transported from central Europe.

The rain trajectories for the non-extreme events show systematically different horizontal transport patterns to the extreme precipitation events. The trajectories approach the target region from the west, north-west or even the north: they do not cross continental Europe or the main basins of the Baltic Sea. Thus, even though our control sample of non-extreme precipitation events was small, the transport patterns were clearly distinct from those shown by the extreme events. This result led us to hypothesise that atmospheric transport over the European continent and the Baltic Sea is an important pre-condition for extreme precipitation in southern Sweden.

The observation that air parcels which precipitate during extreme precipitation events in southern Sweden appear to be transported over Europe and the Baltic, rather than coming directly in from the North Sea, is intriguing. There seems no obvious reason why such pathways should result in more moisture being transported from oceanic source regions, nor why they should result in more powerful uplift over the target region. Thus, we are led back to the hypothesis of Hellström (2005) that regional moisture sources play a significant role in the formation of extreme events in southern Sweden. Indeed, we observe that for most of the extreme events, the specific humidity of air parcels that have been transported from the North Atlantic is usually quite low ($\leq$4 g kg^{-1}) when they reach the European continent. This hypothesis is investigated in the following section.

4. Experiment 2: moisture source region analysis

4.1. A technique to identifying the source region

Displaying the specific humidity along the trajectories gives an indication of where moisture has been gained or lost. This indicated qualitatively that the rain trajectories (the 100 trajectories which lost the largest amount of specific humidity within the target region) gained significant moisture over the Baltic Sea and land surface of the European continent. However, visualizing all the information from all trajectories in this manner is impossible, and in addition we would like a more quantitative analysis. Using a formal definition of the 'source region', and transferring the data to a regular grid, proved to be a much more informative technique for identifying the geographic regions where trajectories gain the most moisture.

A trajectory that runs for 8 days may pick up and lose specific humidity several times before reaching the target region. Therefore, it is important to identify the last cycle of humidity uptake, prior to the final loss in the target region. To determine this region, some rules had to be devised. In this study, the trajectory 'source region' was defined as follows: the specific humidity values for each trajectory at the release point (time 0) were used as a threshold value (Fig. 4). For trajectories where rainfall is occurring in the target region, the specific humidity must have fallen from the time the trajectory entered the target region; with time running backwards, we say that humidity increases away from the release point. Then, the point where the specific humidity falls below the threshold value again for the first time was identified as the starting point of the source region. The maximum specific humidity value between the starting point of the source region and the release point was identified as the end of the source region. This definition gives an amount of humidity uptake corresponding to the loss at the end of the trajectory, although note that not all the loss will occur in the target region.

To extract and visualize the information, hourly changes in specific humidity were calculated for the sections of the trajectories that were identified as source regions, and the data were

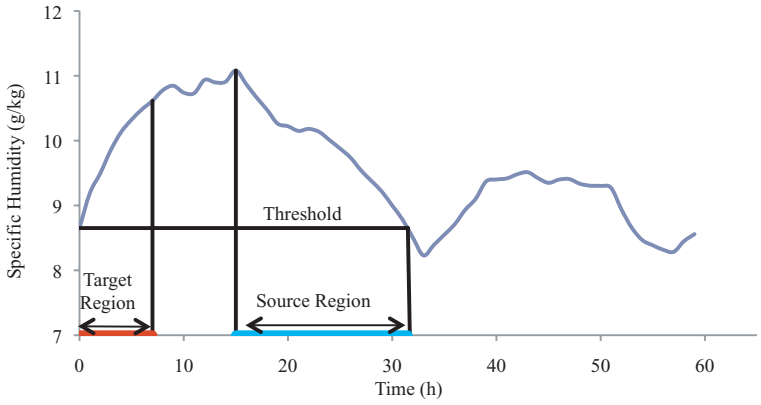

Fig. 4. Illustration of the source region identification rules using an example trajectory. The specific humidity (SH) value at the release point (time = 0 hr) is used as a threshold (8.7 g kg^{-1}), which defines the start of the source region (time = 32 hr). The maximum specific humidity value between the release point and the start of the source region (Max SH = 11g kg^{-1}) defines the end of the source region (time = 15 hr). The target region extent is defined independently (Fig. 1). Note that some of the specific humidity gained in the source region is lost before the trajectory enters the target region.

transferred on to a regular latitude–longitude grid. The hourly changes in specific humidity for all points within each grid cell were summed to give a single value for each grid cell, which was then weighted to reflect the area of the cell. The final result is a grid which shows where the moisture content of the air mass increases for the trajectories that precipitated during a precipitation event.

Using this definition there are, broadly speaking, three factors which may cause a grid cell to be identified as a strong source region. Trajectories may quickly gain a large quantity of moisture, indicating strong evaporation. But even if evaporation is lower, if a large number of trajectories pass over the cell then it will be an important source of moisture. The same is true if trajectories gain moisture over a cell over an extended period.

Using this definition of a source region, there will, however, be some trajectories that lose specific humidity inside the target region but which do not have a defined source region within the 8-day time domain. This is the case where the moisture content along the entire trajectory length remains above the threshold in the target area arrival point. This means that it is uncertain if the moisture lost inside the target region from such trajectories has been picked up within the 8-day time domain or earlier. To examine the importance of the moisture transport from such trajectories, the percentage of specific humidity lost within the target region that could be accounted for by trajectories with defined source regions was calculated. Overall, 92% (varying between 74% and 100% for the different events) of the moisture lost in the target region comes from trajectories that have a source region within the 8-day time domain. The high percentage of moisture accounted suggests that the time domain of 8 days is certainly sufficient for this study, although a shorter time domain may have given a similar percentage. It should also be mentioned that the amount of specific humidity gained inside the identified source regions greatly exceeds, by approximately five times, the total loss inside the target; the excess is rained out as the trajectories approach the target region.

The gridded source region for the extreme event 9 July 1996 (Fig. 2) is shown in Fig. 5, and the source region for the non-extreme event 19 July 1991 (Fig. 3) is shown in Fig. 6. The source regions for all extreme events and non-extreme events are shown in Appendices S3 and S4, respectively, in Supporting Information.

4.2. *Source regions for extreme events*

No two individual events show exactly the same pattern, but the Baltic Sea and continental Europe are clearly important sources of moisture. Some events show very strong increases in specific humidity over small areas, for instance the event on the 18 August 1994 and the event on the 18 August 1970 (Figs. S3r and S3c) which showed strong uptake over the southeast Baltic Sea. Other events showed much less clear patterns with more wide spread source regions, for example on the 11 July 1993 (Fig. S3q) the identified source regions are spread over central Europe all the way down to the Mediterranean, and although an increase occurred over the southern part of the Baltic Sea it is not as strong as for most of the other events. There are also a few events, for example on the 13 July 1972 (Fig. S3e), that gained specific humidity over the central part of Sweden. The events of the 26 August 1979 and the 13 July 1972 (Figs. S3h and S3e) have strong source regions within the Gulf of Bothnia.

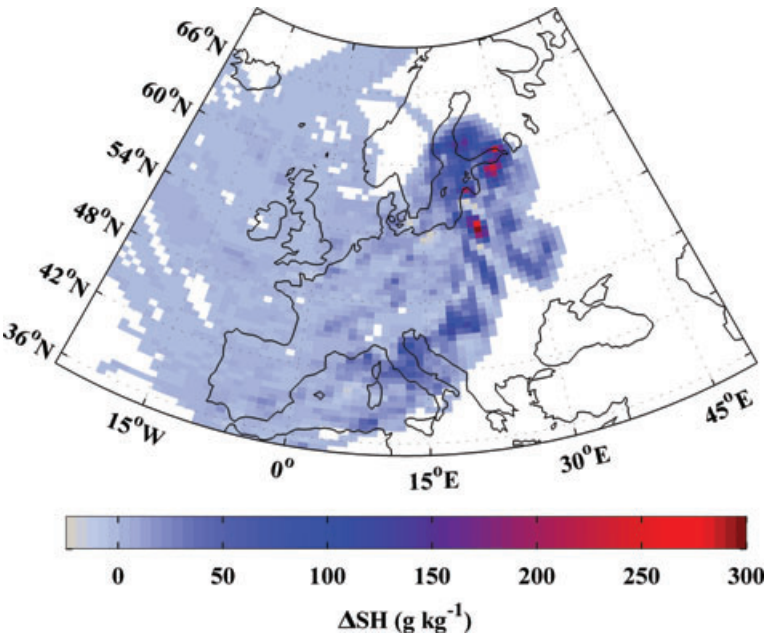

Fig. 5. Source regions for the extreme precipitation event 9 July 1996. Colour scale show the accumulated hourly changes in specific humidity for the sections of trajectories identified as source regions for each grid cell (g kg^{-1}).

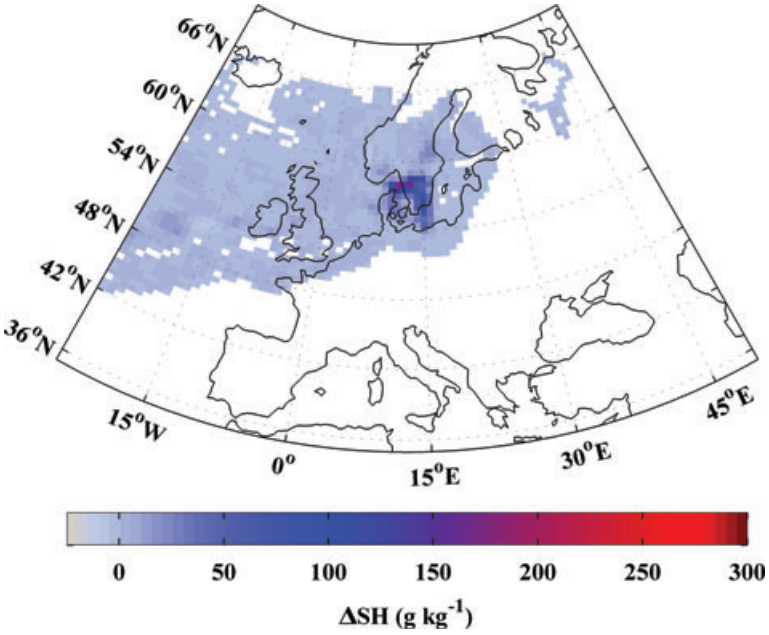

Fig. 6. Source regions for the non-extreme precipitation event 19 July 1991. Colour scale show the accumulated hourly changes in specific humidity for the sections of trajectories identified as source regions for each grid cell (g kg^{-1}).

The patchy patterns of source regions, which can be seen in the individual events, should be treated with caution as they may be a result of the fluctuations in specific humidity along the trajectories. Even if there is a general uptake along the part of a trajectory defined as the source region, the change between 1 hr and the next may be negative. If the occurrences of specific humidity loss coincide geographically for many of the trajectories, then the grid cells representing that region will show a considerable loss in specific humidity, indicating that it is probably raining there. For many of the grid cells, the sum of changes in specific humidity is close to zero.

4.3. Source regions for non-extreme precipitation events

The gridded source regions for the non-extreme events are clearly different from the extreme events, both in the amount of moisture uptake and the spatial distribution. The patterns of source regions for the non-extreme events are much more coherent than for the extreme events, and the general specific humidity uptake is less per grid cell. For the non-extreme events, the regions of strong humidity uptake are all located close to the target region, mostly around the west coast of Sweden, Denmark and over the North Sea. There is only one event—8 June 1989 (Fig. S4e)—where there is substantial moisture uptake over the European continent.

The difference between the source regions of the extreme and non-extreme events is seen most clearly by comparing the combined source regions for the extreme events and the non-extreme events, as in Fig. 7. The combined source regions of the extreme events showed a strong uptake of moisture over the southern half of the Baltic Sea and the coastal land areas of Poland, Kaliningrad, Lithuania and Latvian, a region where the non-extreme events showed low moisture uptake. For the non-extreme events, the Swedish west coast is the most important source of moisture. There were very little uptake over the Baltic Sea and or over central and eastern Europe.

5. Discussion

The rain trajectory paths we calculated for extreme precipitation events consistently passed over the European continent and the Baltic Sea, whereas the rain trajectory paths of the non-extreme rainfall events often did not. This establishes an important characteristic of the atmospheric circulation regime in the lead-up to extreme precipitation events in Southern Sweden.

Our source-region analysis showed that the Baltic Sea and coastal land areas bordering the south-east part of the Baltic Sea are the important source regions for the moisture which rains out as extreme precipitation events over southern Sweden. The importance of 'precipitation recycling', local evaporation feeding into storm systems over the same region, has recently been highlighted for European regions (Bisselink and Dolman, 2009). Schär et al. (1999) performed month-long climate model simulations which showed that summer rainfall levels over Europe were strongly influenced by soil moisture content via associated evapotranspiration. Our results suggest that 'regional precipitation recycling' is an important source of moisture for extreme events in Southern Sweden.

Except for Hellström (2005), the Baltic Sea has not been recognized as an important source of evaporation for extreme rainfall in Sweden. On reflection, this seems an oversight. The summer sea surface temperatures in coastal areas of the Baltic

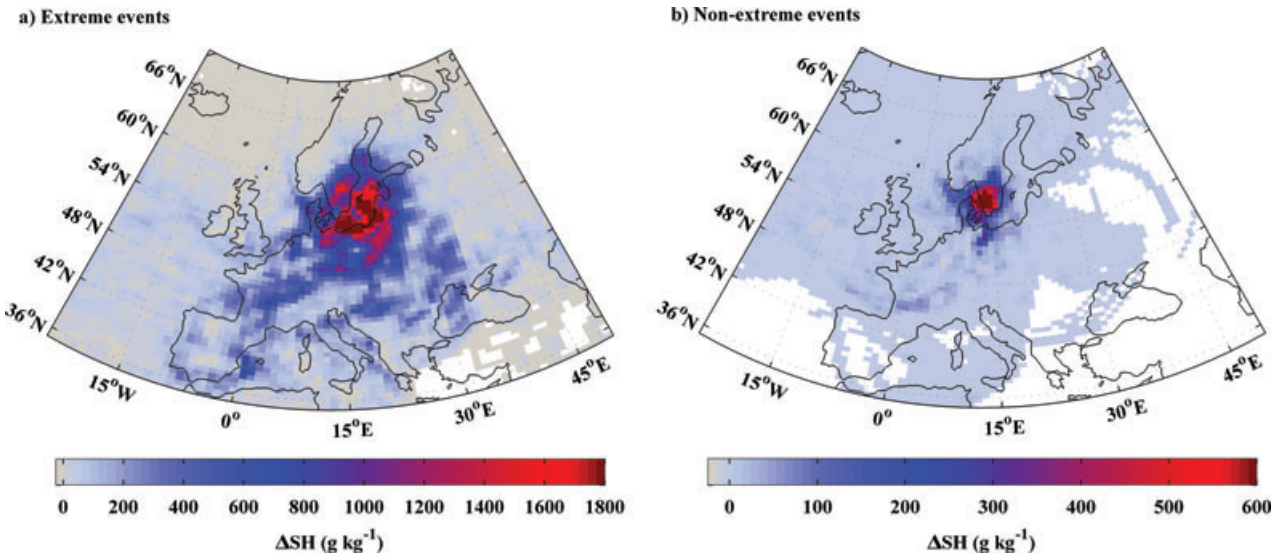

Fig. 7. Combined source regions for (a) extreme events, and (b) non-extreme events. Colour scale show the accumulated hourly changes in specific humidity—for all events—for the sections of trajectories identified as source regions for each grid cell (g kg^{-1}). Note that the colour scales are different for the extreme and the non-extreme events.

Sea may exceed 20 °C due to low levels of mixing of surface water with deeper colder water (Siegel et al., 2006). It is not difficult to imagine that the water content of air flowing across the warm water surface could increase substantially.

It is not possible from our trajectory analysis to make a definite statement about which processes underlie the gain of specific humidity over a specific region. Evaporation or evapotranspiration are the likely sources of moisture, as the specific humidity increases when the air parcels are close to the ground. This suggests that source regions are likely to be areas where air with low vapour-pressure deficit is advected over either water or land with soil moisture available for photosynthesis. Solar radiation falling on the surface would also favour moisture uptake. But to be a 'source region', moisture must be transported out from the atmospheric boundary layer. The extent of turbulent mixing, governed by the wind and specific humidity gradients in the bottom layer of the atmosphere, plays an important role in determining how much moisture can be lifted. It may be that in the coastal areas adjacent to the Baltic Sea, the surface roughness and solar-induced convection are relatively high in summer (compared to the open ocean). As a result, turbulent air flowing from these regions onto the warm Baltic Sea rapidly acquires higher moisture content.

Regarding the technical aspects of our analysis, it became clear during our study that any attempt to use trajectory modelling to define source regions for rainfall events using specific humidity alone faces a fundamental problem. This is that air parcels may gain moisture many times, over different regions, as they travel on their trajectories, and when some of this moisture is lost as precipitation is impossible to say from which of the regions it came. In the future, we may try to overcome this problem by introducing synthetic tracers. For this study, our source region definition connects rainfall to the most recent cycle of moisture gain so as to preferentially select local rather than distance source regions. Even so, the abundance of local moisture sources (with approximately five times more moisture uptake in the source regions than loss inside the target regions); the high fraction of moisture loss in the target region that is associated with trajectories with source regions defined in the 8-day domain; the low specific humidity of the trajectories as they cross the coast; and the identification of highly spatially extended source regions for some extreme events, all together indicate that our conclusion that local moisture uptake is important for extreme events is robust.

6. Conclusions and summary

The work outlined in this paper is a further step towards identifying the critical atmospheric circulation characteristics which lead to extreme events in Southern Sweden. Hellström (2005) recognized the importance of cyclonic weather patterns and southerly winds for extreme event occurrence. Here we provide a more detailed picture, showing that air-masses gain moisture as they cross the European continent and the Baltic Sea prior to extreme-event precipitation. Further, our study suggests where the focus of further investigation into extreme precipitation in Sweden could be directed.

First, we would like to identify the feature/s of the larger-scale atmospheric circulation that result in trajectories crossing the continent and the Baltic before arriving over Sweden. These should be related to the occurrence of extreme precipitation in a quantitative way. Hellström (2005) noted that the zonal flow in

the region is modulated by ridging over western Russia or Finland during extreme events. The trajectory patterns described in this paper are consistent with these observations, especially the dominant pattern where trajectories follow an anti-clockwise pathway over the British Isles, over the northern European continental margin and then north across the Baltic Sea.

Secondly, atmospheric and land/sea-surface conditions could be compared across extreme and non-extreme rainfall events which have similar trajectory profiles. The sample of non-extreme events selected here on the basis of persistent cyclonic Lamb weather type proved to have very different trajectories compared to extreme events with the same weather type classification. Although this is an interesting result, to examine (for example) the role of Baltic Sea temperature or European soil moisture on extreme events will require a set of extreme and non-extreme events with comparable trajectories. Identifying events based on blocking or ridging activity may prove to be an effective way of selecting events with a coherent set of trajectories which can be used for such studies.

In summary, trajectory modelling proved to be a useful method for describing the transport of moisture to extreme summer precipitation in Southern Sweden, and identifying the location of the associated moisture sources. Trajectories contributing to precipitation during extreme events crossed the Baltic Sea or continental Europe before arriving over Sweden, whereas trajectories contributing to precipitation during non-extreme events did not. The change in specific humidity along the trajectories allowed the moisture source regions to be identified, which demonstrated that regional moisture sources around the southern Baltic Sea are important in the formation of extreme precipitation. These results provide a further step towards identifying the critical atmospheric circulation characteristics which lead to extreme events in Southern Sweden, which is in turn necessary for assessing the risk posed by such events, both now and under the future climate.

7. Acknowledgments

The authors are gratefully acknowledge NOAA Air Resources Laboratory (ARL) for the providing the HYSPLIT model; the European Centre for Medium-Range Weather Forecasts (ECMWF) for providing the ERA-40 reanalysis datasets; the NOAA/OAR/ESRL PSD, Boulder, Colorado, USA, for providing the NCEP Reanalysis data; and Alex Walther, University of Gothenburg, for assisting with the Lamb weather class data. The authors thank the three anonymous referees for their comments, which significantly improved this paper.

References

Alexandersson, H. 2006. *Climate Change, a comparison of temperature and precipitation between 1991–2005 and 1961–1990*. In: SMHI information sheet no. 29. (in Swedish), Direkt offset AB, Norrköping, Sweden.

Alexandersson, H. and Vedin, H. 2005. *Extreme Precipitation 1900–2004*. In: SMHI information sheet no. 4. (in Swedish), Direkt offset AB, Norrköping, Sweden.

Achberger, C. and Chen, D. 2006. Trend of extreme precipitation in Sweden and Norway during 1961–2004. Research Report C72, ISSN 1400-383X, Earth Sciences Centre, Göteborg University, Gothenburg, Sweden, 58.

Bisselink, B. and Dolman, A.H. 2009. Recycling of moisture in Europe: contribution of evaporation to variability in very wet and dry years. *Hydrol. Earth Syst. Sci. Discuss.* **6**, 3301–3333.

Bosilovich, M.G. and Schubert, S.D. 2002. Water vapor tracers as diagnostics of the regional hydrological cycle. *J. Hydrometeor.* **3**,149–165.

Browning, K.A. 1997. The dry intrusion perspective of extra-tropical cyclone development. *Meteorol. Appl.* **4**, 317–324.

Chen, D. 2000. A monthly circulation climatology for Sweden and its application to a winter temperature case study. *Int. J. Climatol.* **20**, 1067–1076.

Draxler, R.R. and Hess, G.D. 1998. An overview of the HYSPLIT_4 modeling system for trajectories, dispersion, and deposition. *Aust. Meteor. Mag.* **47**, 295–308.

Draxler, R.R. and Rolph, G.D. 2003. HYSPLIT (Hybrid Single-Particle Lagragnian Integrated Trajectory), Model access via NOAA ARL READY Website NOAA Air Resources Laboratory, Silver Spring, www.arl.noaa.gov/ready/hysplit4.html

Draxler, R.R. 2003. Evaluation of an ensemble dispersion calculation. *J. Appl. Meterol.* **42**, 308–317.

Eckhardt, S., Stohl, A., Wernli, H., James, P., Forster, C. and co-authors. 2004. A 15-year climatology of warm conveyor belts. *J. Clim.* **17**, 218– 237.

Haylock, M.R., Hofstra, N., Klein Tank, A.M.G., Klok, E.J., Jones, P.D. and co-authors. 2008. A European daily high-resolution gridded dataset of surface temperature and precipitation. *J. Geophys. Res (Atmos.)*, **113**, D20119, doi:10.1029/2008JD10201.

Hellström, C. and Malmgren, B. 2004. Spatial analysis of extreme precipitation in Sweden 1961–2000. *Ambio.* **33**, 187–192.

Hellström, C. 2005. Atmospheric conditions during extreme and non-extreme precipitation events in Sweden. *Int. J. Climatol.* **25**, 631–648.

Helsen, M.M., van de Wal, R.S.W., van den Broeke, M.R., Masson-Delmotte, V., Meijer, H.A.J. and co-authors. 2006. Modeling the isotopic composition of Antarctic snow using backward trajectories: Simulation of snow pit records. *J. Geophys. Res.* **111**, 1–19.

Jackson, D.R., Driscoll, S.J., Highwood, E.J., Harries, J.E. and Russell III, J.M. 1998. Troposphere to stratosphere transport at low latitudes as studied using HALOE observations of water vapour 1992–1997. *Q. J. R. Meteorol. Soc.* **124**, 169–192.

James, P., Stohl, A., Spichtinger, N., Eckhardt, S. and Foster, C. 2004. Climatological aspects of the extreme European rainfall of August 2002 and a trajectory methods for estimating the associated evaporative source regions. Nat. Hazards Earth Syst. Sci. 4, 733–746.

Keil, C., Volkert, H. and Majewski, D. 1999. The Oder flood in July 1997: transport routes of precipitable water diagnosed with an operational forecast model. *Geophys. Res. Lett.* **26**, 235–238.

Kalnay, E., Kanamitsu, M., Kistler, R., Collins, W., Deaven, D. and co-authors. 1996. The NCEP/NCAR 40-Year Re-analysis Project. *Bull. Amer. Meteor. Soc.*, **77**, 437–471.

Lamb, H.H. 1950. Types and spells of weather around the year in the British Isles. *Q. J. R. Meteorol. Soc.* **76**, 393–438.

Linderson, M.L., Achberger, C. and Chen, D. 2004. Statistical downscaling and scenario construction of precipitation in Scania, southern Sweden. *Nordic Hydrol.* **35**, 261–278.

Lindström, G. and Bergström, S. 2004. Runoff trends in Sweden 1807–2002. *Hydrol. Sci. J.* 49, 69–84.

Massacand, A.C., Wernli, H. and Davies, H.C. 1998. Heavy precipitation on the Alpine southside: an upper level precursor. *Geophys. Res. Lett.* **25**,1435–1438

Newell, R.E., Newell, N.E., Zhu, Y. and Scott, C. 1992. Tropospheric rivers?—A pilot study. *Geophys. Res. Lett.* **19**, 2401–2404.

Reale, O., Feudale, L. and Turato, B. 2001. Evaporative moisture sources during a sequence of floods in the Mediterranean region. *Geophys. Res. Lett.* **28**, 2085–2088.

Räddningsverket 2000. Översvämning. Document R00 – 222/00, Räddningsverket, Karlstad (in Swedish).

Siegel, H., Gerth, M. and Tschersich, G. 2006. Sea surface temperature development of the Baltic Sea in the period 1990–2004. *Oceanologia* **48**, 119–131.

Schär, C., Lüthi, D., Beyerle, U. and Heise, E. 1999. The soil precipitation feedback: a process study with a regional climate model. *J. Clim.* **12**, 722–741.

Stohl, A. 1998. Computation, accuracy and applications of trajectories – a review and bibliography. *Atmos. Environ.* **32**, 947–966.

Stohl, A., Wotawa, G., Seibert, P. and Kromp-Kolb, H. 1995. Interpolation errors in wind fields as a function of spatial and temporal resolution and their impact on different types of kinematic trajectories. *J. Appl. Meteor.* **34**, 2149–2165.

Stohl, A., Forster, C., Eckhardt, S., Spichtinger, N., Huntrieser, H. and co-authors 2003. A backward modeling study of intercontinental pollution transport using aircraft measurements. *J. Geophys. Res.* **108**(D12), ACH 8-1–ACH 8-18.

Stohl, A., Forster, C. and Sodemann, H. 2008. Remote sources of water vapor forming precipitation on the Norwegian west coast at 60°N a tale of hurricanes and an atmospheric river. *J. Geophys. Res.* **113**, D05102, doi:10.1029/2007JD009006.

Tang, L., Karlsson, P.E., Gu, Y., Chen, D. and Grennfelt, P. 2009. Synoptic weather types and long-range transport patterns for ozone precursors during high-ozone events in southern Sweden. *Ambio*, **38**, 459–464.

Trenberth, K.E. 1998. Atmospheric moisture residence times and cycling: implications for rainfall rates with climate change. *Clim. Change* **39**, 667–694.

Trenberth, K.E. 1999. Atmospheric moisture recycling: role of advection and local evaporation. *J. Clim.* **12**, 1368–1381.

Trenberth, K.E., Dai, A., Rasmussen, R.M. and Parsons, D.B. 2003. The Changing character of precipitation. *Bull. Am. Meteorol. Soc.* **84**, 1205–1217.

Weyhenmeyer, C.E., Burns, S.J., Waber, H.N. and Macumber, P.G. 2002. Isotope study of moisture sources, recharge areas, and groundwater flow paths within the eastern Batinah coastal plain, Sultanate of Oman. *Water Resour. Res.* **38**(10), 1184, doi:10.1029/2000WR000149.

Supporting information

Additional Supporting Information may be found in the online version of this article:

Appendix S1. Stations experiencing extreme events.
Appendix S2. The paths and vertical profiles for the rain-resulting trajectories for all events.
Appendix S3. Gridded source regions for extreme events.
Appendix S4. Gridded source regions for extreme events.

Please note: Wiley-Blackwell are not responsible for the content or functionality of any supporting materials supplied by the authors. Any queries (other than missing material) should be directed to the corresponding author for the article.